Selective Replication of Coronavirus Genomes That Express Nucleocapsid Protein

Barbara Schelle,[1] Nadja Karl,[1]† Burkhard Ludewig,[2] Stuart G. Siddell,[3] and Volker Thiel[2]*

*Institute of Virology and Immunology, University of Würzburg, Würzburg, Germany[1];
Research Department, Kantonal Hospital St. Gallen, St. Gallen, Switzerland[2]; and
Department of Pathology and Microbiology, School of Medical Sciences,
University of Bristol, Bristol, United Kingdom[3]*

The coronavirus nucleocapsid (N) protein is a structural protein that forms a ribonucleoprotein complex with genomic RNA. In addition to its structural role, it has been described as an RNA-binding protein that might be involved in coronavirus RNA synthesis. Here, we report a reverse genetic approach to elucidate the role of N in coronavirus replication and transcription. We found that human coronavirus 229E (HCoV-229E) vector RNAs that lack the N gene were greatly impaired in their ability to replicate, whereas the transcription of subgenomic mRNA from these vectors was easily detectable. In contrast, vector RNAs encoding a functional N protein were able to carry out both replication and transcription. Furthermore, modification of the transcription signal required for the synthesis of N protein mRNAs in the HCoV-229E genome resulted in the selective replication of genomes that are able to express the N protein. This genetic evidence leads us to conclude that at least one coronavirus structural protein, the N protein, is involved in coronavirus replication.

Coronaviruses are enveloped, positive-strand RNA viruses that are mainly associated with enteric or respiratory diseases in humans, companion animals, and livestock. Coronavirus particles contain a genomic RNA of approximately 27,000 to 30,000 nucleotides and four structural proteins: the spike glycoprotein S, the membrane protein M, the small envelope protein E, and the nucleocapsid protein N (44). Three of these four proteins are embedded in the viral envelope. These are the S protein, which mediates binding of the virus particle to the target cell and the subsequent fusion of viral and cellular membranes (8), the M protein, which has a crucial role in the incorporation of the virus nucleocapsid into virus particles (28, 30, 31), and the E protein, which facilitates virus assembly, possibly by inducing curvature into pre-Golgi membranes, the site at which coronaviruses assemble by budding (13, 36). The fourth structural protein, N, is associated with the viral RNA genome to form a ribonucleoprotein complex (38).

The coronavirus N protein has been described as a multifunctional protein displaying RNA-binding activity, protein-protein interaction (specifically with the M protein), and the ability for self-association (22, 29, 30). Clearly, many of these features will reflect the structural role of the N protein in the virus particle. However, there are also some observations that suggest the N protein may have a role in viral RNA synthesis. First, several studies have provided evidence for the binding of N protein to coronaviral RNA sequences that are involved in the regulation of RNA synthesis. These sequences include the coronavirus leader sequence, transcription regulatory sequences (TRS), and sequences corresponding to the 3′ end of coronavirus genomes (2, 10, 11, 24, 34, 48). Second, it has been shown that in addition to a cytoplasmic distribution within the host cell, at least a fraction of the coronavirus N protein colocalizes with replicative proteins at the sites of viral RNA synthesis early in infection (12, 45, 55). Third, it has been demonstrated that there is a requirement for sustained translation of the N protein in *trans* or in *cis* for optimal replication of bovine coronavirus DI RNA and transmissible gastroenteritis virus-derived replicons (1, 9). Fourth, we and others have reported that the recovery of recombinant coronaviruses can be facilitated under conditions that allow sustained N protein expression (7, 59). And fifth, heterologous gene expression from coronavirus-based multigene vectors is greatly improved by cotransfection of vector RNA with a synthetic mRNA encoding the N protein (52).

Coronavirus RNA synthesis can be divided formally into two processes: replication of full-length virus genomes and transcription of subgenomic mRNAs. Genome replication is mediated through a full-length minus-strand copy of the genome that serves as a template for the production of progeny virus genomes. Coronavirus transcription is a complex process involving the discontinuous synthesis of up to eight minus-strand RNAs of subgenomic size which contain sequences corresponding to the 5′ and 3′ ends of the genome and serve as templates for the synthesis of a 5′- and 3′-coterminal set of subgenomic mRNAs (40, 47). According to the current model of coronavirus discontinuous extension, the synthesis of nascent minus-strand RNA initiates at the 3′ end of the plus-strand genomic template and proceeds to TRS elements that are located at various sites within the virus genome (39, 41, 61). At these sites, a proportion of the nascent minus-strand RNA is translocated to the 5′ leader sequence of the genome, and subsequently a minus-strand copy of the leader is added (42,

* Corresponding author. Mailing address: Kantonal Hospital St. Gallen, Research Department, 9007 St. Gallen, Switzerland. Phone: 41-71-4942843. Fax: 41-71-4946321. E-mail: volker.thiel@kssg.ch.

† Present address: Rudolf-Virchow Center for Experimental Biomedicine, 97078 Würzburg, Germany.

57, 61). Thus, the TRS elements determine the fusion sites of leader and "body"-derived sequences (5′- and 3′-end-derived sequences, respectively) of the subgenomic RNAs, and the number of TRS elements correlates with the number of subgenomic mRNAs produced by a particular coronavirus.

In both replication and transcription, proteins encoded by the replicase gene are critically involved. The coronavirus replicase proteins are synthesized as large polyproteins that are extensively processed by virus-encoded proteinases to produce a functional replicase/transcriptase complex (60). It has been suggested that his complex comprises so-called scaffolding proteins, together with proteins that have enzymatic functions, including RNA-dependent RNA polymerase, helicase, and uridylate-specific endoribonuclease (NendoU), and putative exonuclease and 2′-O-ribose methyl transferase activities (44). In addition, the active replicase/transcriptase complex may contain other proteins of viral or cellular origin (17, 21, 26, 27, 43, 44). These proteins might include the N protein. On the other hand, Snijder and colleagues have shown that all structural proteins of the closely related arterivirus equine arteritis virus, including the N protein, are dispensable for genome replication and subgenomic RNA synthesis (25); we have shown that the viral replicase gene products alone suffice for coronavirus transcription (50).

In this paper, we used a reverse genetic approach to study N protein function in the context of viral RNA synthesis. Our data suggest a role for the coronavirus N protein in virus replication. We show that efficient, sustained replication of coronavirus-based vector RNAs only takes place if the N protein is expressed by the vector RNA. We also show that the level of N protein expression determines the level of vector RNA-mediated reporter gene expression, which again is consistent with a role for N in vector RNA replication. And finally, by constructing and monitoring the replication of recombinant, mutated coranavirus genomes, we provide genetic evidence that sustained expression of the N protein facilitates replication of the genomic RNA.

MATERIALS AND METHODS

Viruses and cells. BHK-21 and CV-1 cells were purchased from the European Collection of Cell Cultures. D980R cells were a kind gift from G. L. Smith, Imperial College, London, United Kingdom. All cells were maintained in minimal essential medium supplemented with fetal bovine serum (5 to 10%) and antibiotics. Recombinant vaccinia viruses were propagated, titers were determined, and the viruses were purified as previously described (49).

Cloning of plasmid DNAs and recombinant vaccinia viruses. The isolation of recombinant vaccinia viruses vHCoV-vec-1, vHCoV-vec-CLG, and vHCoV-vec-GN has been described previously (15, 50, 52). The isolation of recombinant vaccinia virus vHCoV-SfiI is based on the recombinant vaccinia virus vHCoV-inf-1, which contains the full-length cDNA of the human coronavirus 229E (HCoV-229E) genome (49). The first step, the generation of recombinant vaccinia virus vRec-1, has been described previously (15). The genome of vaccinia virus vRec-1 contains a cDNA insert corresponding to HCoV-229E nucleotides (nt) 1 to 21145, followed by a 2.1-kbp DNA fragment containing the *Escherichia coli* guanine phosphoribosyltransferase gene (*gpt*) under the control of a vaccinia virus promoter and a cDNA fragment corresponding to the 3′ end of the HCoV-229E genome, starting at nt 24646. The second step involved homologous recombination of vRec-1 DNA with pHCoV-SfiI DNA and the isolation of vaccinia virus vHCoV-SfiI using *gpt*-negative selection in D980R cells. To clone the plasmid pHCoV-SfiI, a PCR product corresponding to HCoV-229E nt 20478 to 24091 was generated using primers SacI-20500up (5′-ACGTGAGCTCGGTGC TTAGTCTTGTTAGGAGTGG-3′) and StopS-Sndown (5′-ACGTGCGGCCG CGGCCATTACGGCCTTACTGTATGTGGATCTTTTCAACG-3′) and vHCoV-inf-1 DNA as a template. The PCR product was cleaved with SacI and NotI

and cloned in pBluescriptII KS(+) (Stratagene). The resulting plasmid DNA was cleaved with NotI and HindIII, and a NotI-HindIII DNA fragment derived from NotI-HindIII-cleaved vaccinia virus vNotI/tk (23) genomic DNA (corresponding to the DNA sequence located downstream of the 3′ end of the HCoV-229E genome in the vaccinia virus vRec-1 genome) was inserted. The identity of pHCoV-SfiI was confirmed by sequencing analysis and used for homologous recombination with vRec-1 DNA to generate the recombinant vaccinia virus vHCoV-SfiI. Note that the HCoV-229E-derived sequence of vHCoV-SfiI encompasses the HCoV-229E nt 1 to 24091 (nt 24089 to 24091 represent the stop codon of the HCoV-229E S gene), followed by a SfiI restriction site which is unique in the vHCoV-SfiI genome.

To construct the plasmid pMHV-N, cDNA was amplified by RT-PCR using primer Sac-MN-ATG (5′-ACGTAGACTCACCATGTCTTTTGTTCCTGGGC AAGAAAATGC-3′), primer Bam-MN-stop (5′-ACGTGGATCCTTACACAT TAGAGTCATCTTCTAACC-3′), and vMHV-inf-1 DNA (9a). as a template. The resulting PCR product, which contains the mouse hepatitis virus (MHV) N gene, was cleaved with SacI and BamHI and cloned into pBluescriptII KS(+).

To construct the plasmid pTRE-HN, the HCoV-229E N gene was amplified by PCR using the oligonucleotide primer SacII-HN-ATG (5′-ACGTAGAGCTCA CCATGGCTACAGGTCAAA TGGGCTGATGC-3′, primer Bam-HN-Stop (5′-ACGTGGATCCTTAGTTTACTTCATCAATTATGTCAG-3′), and vHCoV-inf-1 DNA as a template. The PCR product was cleaved with SacII and BamHI and ligated into the SacII- and BamHI-cleaved plasmid pTRE DNA.

Generation of synthetic N protein cDNA templates for in vitro transcription. Plasmid pME (49) was used as template to generate a PCR product containing the HCoV-229E N gene using primers Nup (5′-ACGTAATACGACTCACTA TAGGGACGAAACCATGGCTACAGTC AAATGGGCTG-3′) and Ndown (5′-TTTTTTTTTTTTTTTTTTTTTTCAAACAACACAGTGGCA TGTTTAG-3′). The PCR product was used as template for in vitro transcription of a mRNA encoding the HCoV-229E N protein. Plasmid pMSN was a kind gift of M. Ackermann and K. Tobler, Department of Veterinary Medicine, University of Zürich, Zürich, Switzerland, and contains the porcine epidemic diarrhea virus (PEDV) N gene located downstream of a bacteriophage T7 RNA polymerase promoter. pMSN was linearized with NotI prior to in vitro transcription of a synthetic mRNA encoding the PEDV N protein. Plasmid pMHV-N was linearized with XhoI prior to in vitro transcription of a synthetic mRNA encoding the MHV N protein.

Generation of a stable cell line expressing the HCoV-229E N protein. To generate a stable cell line expressing the HCoV-229E N protein, BHK-21 cells were transfected with 5 μg of plasmid pcEF$_{Tet-On}$/NEO (37) and a stable cell line, designated BHK-Tet/On, which expresses the Tet-activator protein rtTA, was selected using G418 (400 to 800 μg/ml). BHK-Tet/On cells were transfected with 2.5 μg of plasmid pTRE-HN and 2.5 μg of plasmid pTK-Hyg (Clontech); a stable cell line, BHK-HCoV-N, expressing the HCoV-229E N protein in the presence of doxycyclin, was selected with hygromycin B (300 μg/ml). N protein expression in BHK-HCoV-N cells was analyzed by Western blotting using murine monoclonal antibody NG12 (16) as primary antibody and NA 931 (sheep anti-mouse immunoglobulin G, peroxidase-linked; Amersham) as secondary antibody in combination with ECL Western blotting detection reagents (Amersham), according to the manufacturer's instructions.

Generation of recombinant HCoV-229E cDNA containing randomized sequences. A DNA fragment containing the HCoV-229E-derived nt 24097 to 27277 with a randomized sequence at HCoV-229E nt 25671 to 25673 was generated. Two PCRs were carried out with plasmid pME as template and primers (i) Oli 17 (5′-TGTGGTGAGTATGTTGCT-3′) and EspTRSNr-down (5′-ACG TCGTCTCTTCAGNNNAGAAAAAATGAAGCAATCTTTCGTTTTCTGT C-3′; N represents any nucleotide) or (ii) EspTRSNr-up (5′-ACGTCGTCTCC CTGAACGAAAAGATGGCTACAGTCAAATGGGC-3′) and Hend-polyA (5′-TTTTTTTTTTTTTTTTTTTTTTTTGTGTATCCATATCGAAACCGTTCC-3′). Both PCR products were cleaved with Esp3I, then ligated in vitro, and used as a template for another PCR with primers Sfi4a-up (5′-ACGTGGCCGTAATG GCCCTAGGTTTGTTCACATTGCAACTTGTG-3′) and Hend-polyA. The resulting PCR product contains HCoV-derived nt 24097 to 27277 (with randomized nt 25671 to 25673) plus a SfiI cleavage site and a poly(A) sequence encoded upstream and downstream, respectively. After cleavage with SfiI, the DNA fragment was ligated in vitro with Sfi-cleaved genomic DNA from purified recombinant vaccinia virus vHCoV-SfiI, and the resulting ligation product was used as template for bacteriophage T7 RNA polymerase-driven in vitro transcription.

In vitro transcription and electroporation. In vitro transcription using bacteriophage T7 RNA polymerase in the presence of an m7G(5′)ppp(5′)G cap analog was done as described previously (49). Vector RNA (15 μg) or full-length recombinant HCoV-229E RNA was electroporated as previously described (50) into BHK-HCoV-N or BHK-21 cells with or without 5 μg in vitro-transcribed

RNA encoding the HCoV, PEDV, or MHV N proteins. A synthetic mRNA encoding a truncated *E. coli* β-galactosidase protein has been described previously (54), and 5 μg was used as a negative control for electroporation.

Reporter protein analysis. Reporter protein expression was analyzed 3 days postelectroporation. Green fluorescent protein (GFP) expression was analyzed by fluorescence microscopy with a Leica DM IL fluorescence microscope and flow cytometry was analyzed wtih a FACSCalibur and CellQuest software (BD Biosciences). Sorting of green fluorescent BHK-21 cells that were transfected with HCoV-vec-1 RNA and HCoV-229E-N mRNA was done using a FACS-Vantage Instrument (BD Biosciences). Firefly luciferase expression was analyzed using the luciferase reporter gene assay (Boehringer, Mannheim, Germany), as described by the manufacturer.

RNA preparation, Northern blotting, RT-PCR, and sequencing analysis. Poly(A)-containing RNA was isolated from BHK-21 cells using oligo(dT)$_{25}$ Dynabeads (Dynal, Oslo, Norway) as previously described (53). Northern blot analysis involved electrophoresis and transfer to nylon membranes as previously described (51). To detect HCoV-229E-specific RNAs, a ^{32}P-labeled probe corresponding to the HCoV-229E nucleotides 26297 to 27273 was produced using the Multiprime DNA-labeling system (Amersham). Reverse transcription-PCR (RT-PCR) was done with Superscript II reverse transcriptase (Invitrogen) as described previously (53). To amplify the region containing the HCoV-229E TRS-N region by RT-PCR, in vitro transcripts or poly(A)-containing RNA from transfected cells was used as a template for reverse transcription with primer 25950-down (5′-GCATCTTTATGGGGTCCTGTGCC-3′). The RT products were used as templates to amplify the TRS-N region corresponding to the HCoV-229E genome and subgenomic N protein mRNAs using (semi)nested PCR protocols. To amplify the TRS-N region corresponding to recombinant HCoV-229E genomes, primers 25500-up (5′-CATGACAGTTGCCGTGCCGA GCAC-3′) and 25900-down (5′-TGACAAATCCACCCGTTTGCCCT-3′) were used for the first PCR; primers 25630-up (5′-CTGCAGTGAGCTCTCCCATG AGCA-3′) and 25820-down (5′-GTCTTTCTTGTTGATGGGTACC-3′) were used for the nested PCR. To amplify the leader-body junction of N protein mRNAs, the leader-specific primer 25-up (5′-CTTAAGTACCTTATCTATCT ACAGATAG-3′) and primer 25900-down were used for the first PCR, and primers 25-up and 25820-down were used for the seminested PCR. The resulting PCR products were analyzed directly by sequencing using primer 25820-down or cloned into plasmid pGem-T (Promega). The resulting plasmid clones have been sequenced to determine the sequence of individual genomic or subgenomic mRNAs at the TRS-N region. Sequencing analysis of plasmid DNA, RT-PCR products, and the recombinant vaccinia virus cDNA inserts was done by standard cycle sequencing methods with an ABI 310 Prism Genetic Analyzer. Computer-assisted analysis of sequence data was facilitated by the Lasergene bio-computing software (DNASTAR).

RESULTS

Cotransfection of HCoV-229E vector RNAs with N protein mRNAs. The aim of this study was to analyze the coronavirus N protein function(s) that might be related to viral RNA synthesis by using a reverse genetic approach based on HCoV-229E. The recombinant RNA constructs used in this study are illustrated in Fig. 1. We previously reported that transfection of a HCoV-based vector RNA, designated HCoV-vec-1, into BHK-21 cells resulted in the synthesis of a subgenomic mRNA that contained a leader-body fusion site characteristic of coronavirus transcription (50). These data indicate that the replicase gene products suffice for coronavirus transcription because the only viral proteins encoded by the HCoV-vec-1 RNA are derived from the replicase gene. Similar results have been obtained using another vector RNA, designated HCoV-vec-CLG (52). We have also reported that after transfection of GFP-encoding HCoV-229E-based vector RNAs (HCoV-vec-1 or HCoV-vec-CLG) only very few transfected cells (<0.1%) displayed green fluorescence. However, if a synthetic mRNA encoding the HCoV-229E N protein was cotransfected with HCoV-vec-CLG RNA, we found that the percentage of green fluorescent cells increased up to 3%. When we used a synthetic RNA where the AUG start codon of the N protein gene was
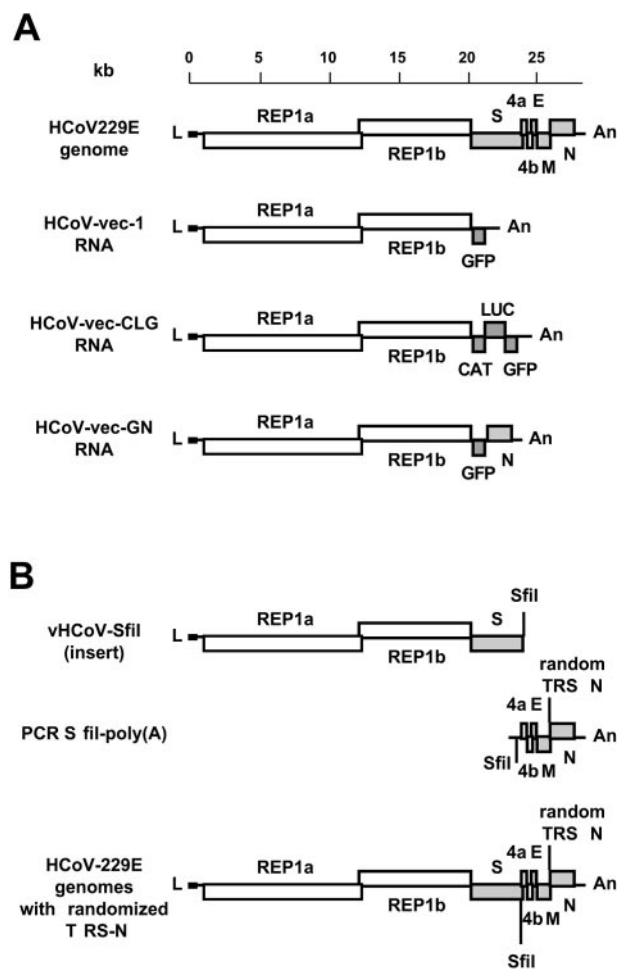

FIG. 1. Structure of recombinant HCoV-229E and vector RNAs. (A) The structural relationship and sizes of HCoV-229E and vector RNAs used in this study are shown. Open reading frames are indicated as boxes designated by encoded gene products. L, leader RNA sequence; An, poly(A) sequence. (B) The structure of recombinant HCoV-229E genomes with a randomized N gene TRS is shown (bottom). Also shown are the cDNAs that have been ligated in vitro (at the SfiI site) to produce a full-length HCoV-229E cDNA template for in vitro transcription.

changed to CCG, we again observed <0.1% of green fluorescent cells after cotransfection with HCoV-vec-CLG RNA (52). This indicates that the N protein rather than the N mRNA sequence is responsible for the observed effect.

Based on these observations, we constructed a vector DNA, designated HCoV-vec-GN, that transcribes to produce an RNA containing the N protein gene in addition to the HCoV-229E replicase gene and the GFP reporter gene (Fig. 1). The N gene in HCoV-vec-GN is located downstream of the GFP gene, and transcription of an N gene mRNA is driven by the authentic TRS-N region, corresponding to the HCoV-229E nt 25654 to 25685 (including the TRS-N core sequence ^{25668}UC UAAACU^{25675}). As shown in Fig. 2, transfection of HCoV-vec-GN RNA into BHK-21 cells resulted in <0.1% green fluorescent cells. In contrast, cotransfection of a synthetic mRNA encoding the HCoV-229E N protein together with
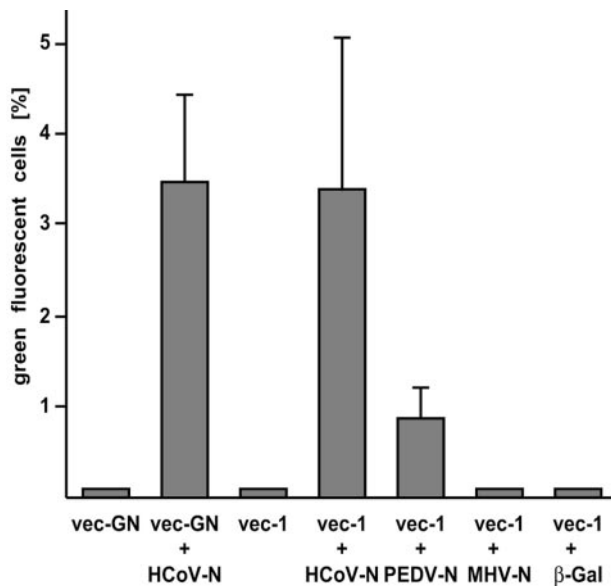
FIG. 2. Transfection of vector RNAs. Vector RNA HCoV-vec-GN or HCoV-vec-1 (each, 15 μg) was transfected into BHK-21 cells with or without synthetic mRNAs (5 μg) encoding the HCoV-229E, PEDV, or MHV N proteins or a truncated β-galactosidase protein as indicated. Three days posttransfection, the percentage of green fluorescent cells was analyzed by flow cytometry. Each column represents the mean value of three independent experiments.

HCoV-vec-GN RNA resulted in an increased number of green fluorescent cells (3.5%). These cells displayed relatively intense fluorescence 16 h posttransfection. This contrasts with the result observed when HCoV-vec-1 RNA (which does not encode the HCoV-229E N protein) was cotransfected with the mRNA encoding the HCoV-229E N protein. Again, an elevated number of green fluorescent cells (3.4%) (Fig. 2) were seen, but in this case the intensity of fluorescence was lower and only became apparent 48 h posttransfection. To show that the elevated percentage of green fluorescent cells did not result from the cotransfection of any RNA, we cotransfected mRNA encoding a truncated *E. coli* β-galactosidase protein with the HCoV-vec-1 RNA. Again, <0.1% of green fluorescent cells were detected (Fig. 2).

Thus, we conclude that cotransfection of mRNA encoding the HCoV-229E N protein with HCoV-229E-based vector RNAs encoding GFP increased the number of green fluorescent cells. Even if the N protein was encoded by the vector RNA itself, the number of GFP-expressing cells remained at a low level when the vector RNA was transfected alone. These results show that the presence of N protein early after transfection of vector RNAs (i.e., N protein that is provided in *trans*) enhances the level of coronavirus-mediated subgenomic mRNA transcription. However, they do not allow us to conclude whether this is due to increased transcription from templates derived from the input vector RNA or from de novo synthesized (i.e., replicating) vector RNA.

Next, we asked whether the N proteins of other coronaviruses could provide the same *trans*-active function(s) as the HCoV N protein in the system described above. Thus, we produced two further synthetic mRNAs encoding the MHV and PEDV N proteins, respectively. As shown in Fig. 2, co-

transfection of HCoV-vec-1 RNA with mRNAs encoding the MHV or PEDV N proteins resulted in <0.1 and 0.9% green fluorescent cells, respectively. We conclude that only the PEDV N protein mRNA gave rise to an increased number of green fluorescent cells, although less effectively than the HCoV-229E N protein mRNA. Notably, PEDV is a group I coronavirus and closely related to HCoV-229E (6, 20), whereas MHV is a group II coronavirus and more distantly related to HCoV-229E.

Detection of HCoV-229E vector-specific RNAs by Northern blot analysis. In addition to measuring the levels of GFP expression, we also used a ^{32}P-labeled probe, corresponding to the 3′ end of the HCoV-229E genome, to visualize the vector-specific RNAs produced in transfected cells. Despite using probes of high specific activity, we were not able to detect any RNAs from cells that were transfected with HCoV-vec-1 or HCoV-vec-GN vector RNA alone. After cotransfection of HCoV-229E N mRNA with HCoV-vec-1 RNA, we could detect a faint signal for a subgenomic mRNA encoding GFP (data not shown). This contrasted with the cotransfection of HCoV-229E N mRNA with HCoV-vec-GN RNA, where we could easily detect the vector RNA and two mRNAs encoding GFP and N protein (Fig. 3, lane 11). In order to increase the sensitivity of RNA analysis from cells that have been transfected with HCoV-229E N mRNA and HCoV-vec-1 RNA, we sorted the green fluorescent cells prior to the isolation of poly(A)-containing RNA. In this case, an RNA that corresponds to a subgenomic mRNA encoding GFP was easily detectable (Fig. 3, lane 7), but we were unable to detect full-length HCoV-vec-1 RNA (Fig. 3, lane 10), even after prolonged autoradiography.

To exclude degradation or the incomplete transfer of full-length HCoV-vec-1 RNA during RNA preparation, gel electrophoresis, or Northern blotting, we also applied poly(A)-containing RNA from HCoV-229E-infected cells (Fig. 3, lane 1) and 1 ng of in vitro-transcribed HCoV-vec-1 RNA and HCoV-vec-CLG to the same gel (Fig. 3, lanes 3 and 4, respectively, and the corresponding lanes 8 and 9 after prolonged autoradiography). In each case, virus and vector RNAs were detectable, irrespective of their size. To exclude that the RNA detected in HCoV-vec-1 and HCoV-229E N mRNA-transfected cells corresponded to the transfected N protein mRNA, we applied 1 ng of in vitro-transcribed N protein mRNA (i.e., used for cotransfection with HCoV-vec-1 RNA) to the same gel. This RNA was also easily detectable (Fig. 3, lane 5) and, consistent with its smaller size, migrated faster in the gel than the subgenomic mRNA detected in HCoV-vec-1-transfected cells.

These results show that vector RNAs encoding a functional N gene were able to transcribe and replicate RNA, whereas vector RNAs lacking the N gene were able to transcribe RNA but replication of full-length vector RNA was not detectable. However, these results cannot rigorously rule out the possibility that the N gene provides a *cis*-acting RNA signal that enhances replication. To address this question, we coelectroporated the HCoV-vec-CLG vector RNA (lacking the N gene) with recombinant full-length virus genome and an mRNA encoding the N protein into BHK-21 cells. In this case, rapidly available N protein was supplied by translation of the cotransfected N protein mRNA and sustained N protein expression
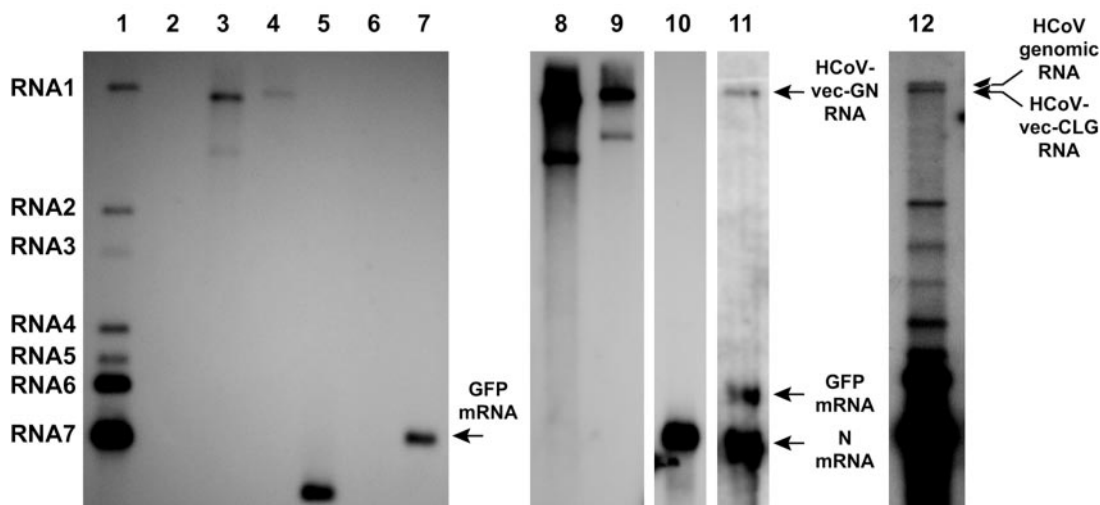
FIG. 3. Northern blot analysis. Poly(A)-containing RNA was isolated from HCoV-229E-infected MRC-5 cells (lane 1), BHK-21 cells (lane 6), BHK-21 cells that have been transfected with HCoV-229E N protein mRNA and HCoV-vec-1 RNA (lanes 7 and 10), BHK-21 cells that have been transfected with HCoV-229E N protein mRNA and HCoV-vec-GN RNA (lane 11), or BHK-21 cells that have been transfected with HCoV-229E N protein mRNA, HCoV-vec-CLG RNA, and HCoV-229E genomic RNA (lane 12). The RNA was analyzed by Northern blotting as described in Materials and Methods. Lane 2, no RNA; lanes 3 and 8, 1 ng of in vitro-transcribed HCoV-vec-1 RNA; lanes 4 and 9, 1 ng of in vitro-transcribed HCoV-vec-CLG RNA; lane 5, 1 ng of in vitro-transcribed HCoV-229E N protein mRNA. Lanes 8, 9, and 10 represent lanes 3, 4, and 7, respectively, after prolonged autoradiography. Genomic and subgenomic RNAs of HCoV-229E (RNA1 to -7) and HCoV-229E vector RNAs (arrows) are indicated.

was mediated by the full-length genomic RNA in *trans*. Again, 3 days posttransfection we analyzed poly(A)-containing RNA from transfected cells by Northern blotting. As shown in Fig. 3, lane 12, the full-length HCoV-vec-CLG RNA is readily visible, indicating that replication of vector RNA in the presence of replicating HCoV-229E virus had occurred. In summary, our data indicate that initially, after transfection of vector RNAs, the N protein (provided by cotransfected N protein mRNA) may be important for the establishment of a replicase/transcriptase complex; however, sustained N protein expression (e.g., if the N protein was encoded by the vector RNA itself or provided in *trans* by replicating virus) was required for efficient replication.

The level of HCoV-229E vector-mediated reporter gene expression correlates with the level of HCoV-229E N protein expression. The experiments described above demonstrate that cotransfection of an HCoV-229E N protein mRNA with HCoV-229E vector RNAs increases the number of green fluorescent cells. Even if the N protein is encoded by the vector RNA, cotransfection of an N protein mRNA is required, indicating that the N protein must provide a function that facilitates the establishment of a functional transcriptase or replicase complex early after transfection. To determine whether this effect was dose dependent, we produced a stable, regulatable BHK-21-derived cell line expressing the HCoV-229E N protein. This cell line, designated BHK-HCoV-N, is based on the Tet/ON system. The analysis of N protein expression by Western blotting revealed that the HCoV-229E N protein can be expressed to different levels with different concentrations of doxycyclin in the tissue culture medium (Fig. 4A). We have used this cell line for the transfection of 15 μg in vitro-transcribed HCoV-vec-CLG RNA and analyzed the vector-mediated expression of GFP and firefly luciferase 3 days posttrans-

fection. The average percentage of green fluorescent cells in these experiments was approximately 3%, independent of the doxycylin concentration used in the medium (data not shown). This indicates first that cotransfection of an mRNA encoding the N protein with the vector RNA is no longer needed in N protein-expressing cells, and second, that the level of N protein expression did not influence the number of green fluorescent cells. However, as shown in Fig. 4B, the level of N protein expression did influence the level of reporter protein expression. At doxycyclin concentrations of 0.1 and 1 μg/ml, the firefly luciferase expression was about 30-fold higher than levels observed with HCoV-vec-CLG RNA-transfected cells in the absence of doxycyclin. Thus, although the overall number of green fluorescent cells did not change, the level of reporter protein expression increased at higher levels of N protein expression.

Selection of replication-competent HCoV genomes. Having shown that the HCoV-229E N protein provides a function that increases the number of green fluorescent cells and the level of reporter protein expression after transfection of HCoV-229E-based vector RNAs, we asked whether the N protein is involved in coronavirus replication or coronavirus transcription. As mentioned above, we were unable to detect efficient vector RNA replication when the N protein was not encoded by the vector RNA (Fig. 3, lanes 7 and 10). However, as soon as sustained N protein expression was ensured, full-length vector RNAs became detectable by Northern blot analysis (Fig. 3, lanes 11 and 12). Accordingly, we reasoned that HCoV-229E genomes do not replicate efficiently if they are unable to mediate N protein expression. To test this hypothesis, we decided to analyze the replication of HCoV-229E genomes that had been modified at the TRS of the N gene (TRS-N), a *cis*-acting
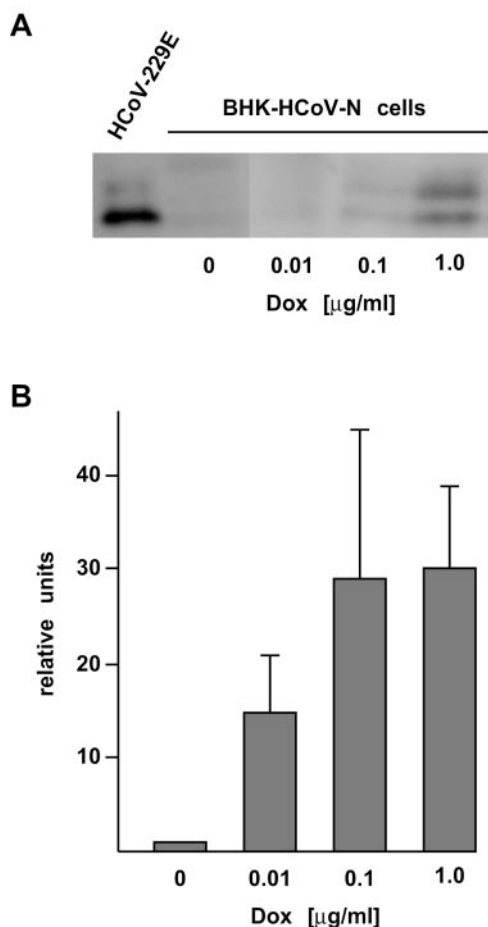
FIG. 4. Firefly luciferase reporter protein analysis in BHK-HCoV-N cells. (A) Western blot analysis of BHK-HCoV-N cells. Each lane corresponds to a cytoplasmic lysate derived from 2×10^5 BHK-HCoV-N cells that were cultivated for 2 days in medium without or with 0.01, 0.1, or 1 μg/ml doxycyclin (Dox), as indicated. For comparison, a Western blot analysis of cytoplamic lysate derived from 2×10^5 HCoV-229E-infected MRC-5 cells is shown. (B) A total of 15 μg of HCoV-vec-CLG vector RNA was transfected into 10^7 BHK-HCoV-N cells. After transfection, the cells were split into four wells containing medium without or with 0.01, 0.1, or 1 μg/ml Dox. Luciferase activity was analyzed 3 days posttransfection. Results are shown for three independent experiments. In each experiment, luciferase activity of transfected BHK-HCoV-N cells that were cultivated without Dox were set as 1 relative unit. Bars indicate 95% confidence intervals.

RNA element which is required for the production of a subgenomic mRNA encoding the N protein.

The fusion of leader and body-derived sequences of the subgenomic HCoV-229E N protein mRNA has been determined to occur at the TRS-N sequence ^{25668}UCUAAACU^{25675} (the numbers indicate HCoV-229E nucleotide positions) within the HCoV-229E genome (14). We made use of our full-length cDNA clone of HCoV-229E and modified the TRS-N to ^{25668}UCUNNNCU^{25675}, where N represents any nucleotide (Fig. 5A). The stretch of three random nucleotides within the TRS-N was introduced into a full-length cDNA of HCoV-229E by PCR and in vitro ligation as described in Materials and Methods. Following in vitro transcription, a population of (theoretically) 64 different full-length recombinant

HCoV-229E genomes was produced. These RNA molecules were then transfected into BHK-21 cells (which are not susceptible to HCoV-229E infection), and 3 days later poly(A)-containing RNAs were isolated. We then compared the sequences of the input RNA genomes with those of the reisolated RNA genomes at the TRS-N region. To do this, DNA fragments containing the TRS-N region were amplified by RT-PCR from the RNA genomes, and a consensus sequence was determined. As shown in Fig. 5B, the reisolated RNA genomes have clearly undergone selection, since the nucleotides at the randomized positions had shifted to a predominance of adenines. However, there was also a dominant uridine peak detectable, corresponding to HCoV-229E nt 25673. To determine the sequences of individual RNA genomes, we cloned the RT-PCR products and sequenced a total of 44 plasmid DNAs derived from the input RNA population and 41 plasmid DNAs derived from the reisolated RNA population. The result of this analysis is summarized in Fig. 5C. HCoV-229E genomes that contained the authentic TRS-N sequence were represented at 4.5% in the input RNA population, and the percentage of these molecules increased to 9.8% in the reisolated RNA population. Similarly, the percentage of genomes that contained a uridine at position 25673 was 20.5% of the input RNAs and 41.5% of the reisolated RNAs. Thus, these two groups had obviously undergone positive selection during amplification in BHK-21 cells. Sequences that contained one nucleotide difference, compared to the authentic TRS-N (^{25668}UCUAAACU^{25675}) or leader-TRS (^{62}UCUCAACU^{69}), remained approximately at the same level (31.8% and 29.3% for input and reisolated RNAs, respectively). Other sequences that did not match to the groups mentioned above had presumably undergone negative selection in BHK-21 cells, since their percentage dropped from 43.2% in the input RNAs to 19.5% in the reisolated RNAs.

Analysis of subgenomic N protein mRNAs. The finding that specific HCoV-229E genomes within the transfected population had undergone positive selection in nonsusceptible BHK-21 cells indicates that these genomes were replicated preferentially. If this phenotype is related to the ability to transcribe N protein mRNA, it should be possible to find N protein subgenomic mRNAs; furthermore, the sequence at the randomized TRS-N positions of these mRNAs should correlate with the sequences of the selected genomes. Therefore, we did an RT-PCR to specifically amplify N protein mRNAs that had been produced in the transfected cells. Using a leader RNA-specific primer and a body RNA-specific primer in the PCR, we were able to obtain RT-PCR products from reisolated poly(A)-containing RNAs that corresponded to N protein mRNAs. These products were cloned, and the sequences at the leader-body fusion sites were determined (Fig. 6). As expected, most N protein mRNAs (>60%) contained either the authentic TRS-N sequence (UCUAAACU) or the sequence corresponding to the leader TRS (UCUCAACU), confirming that these TRS elements were efficient in directing the synthesis of coronavirus subgenomic mRNAs. Also as expected, the authentic N protein mRNA leader-body fusion site was used when these sequences were present. Similarly, the authentic leader-body fusion site was present in three N protein mRNAs that contained only one nucleotide change compared to the leader or N gene TRSs (one of these sequences,
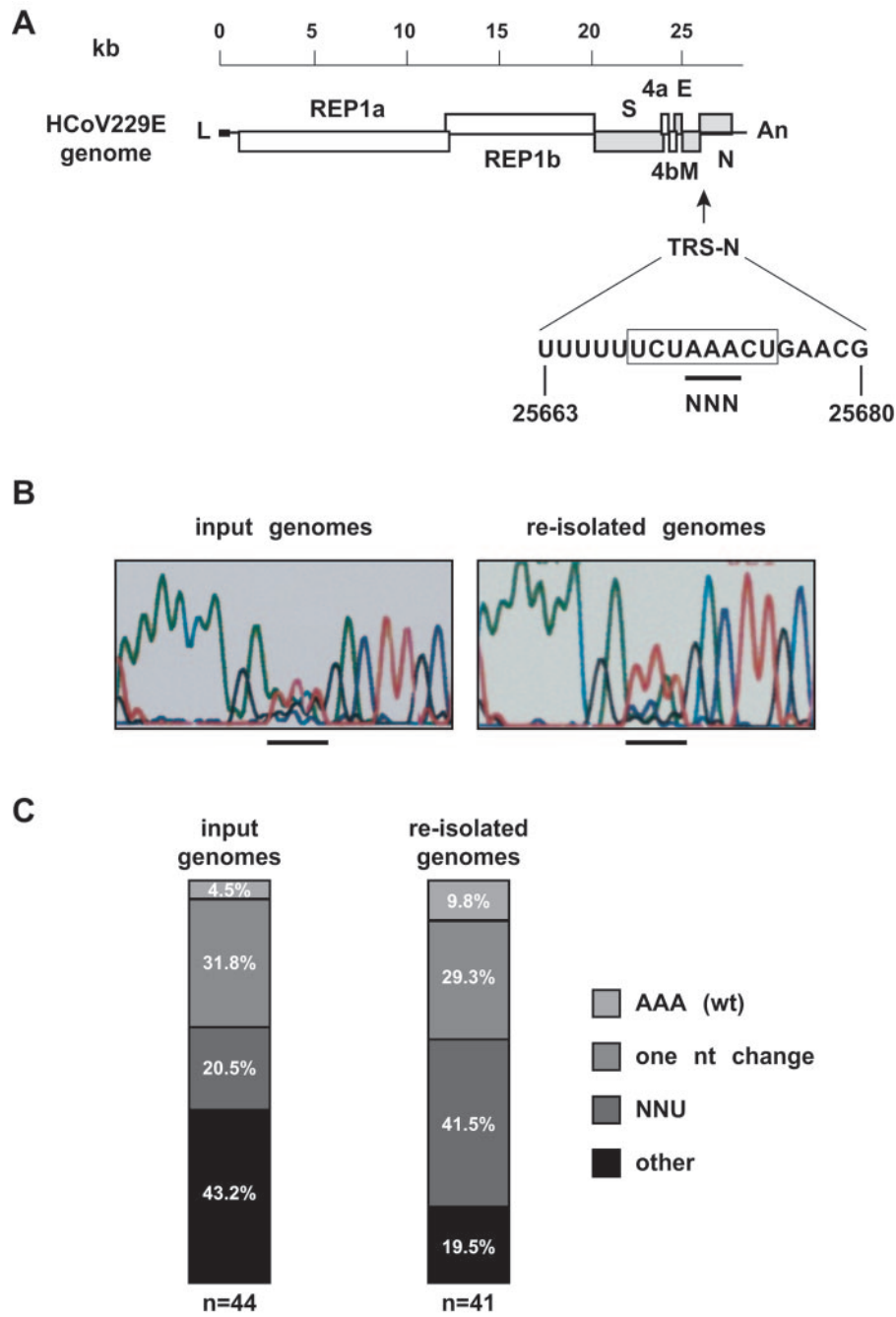
FIG. 5. Sequencing analysis of recombinant HCoV-229E genomes with a randomized N gene TRS. (A) HCoV-229E nt 25663 to 25680 containing the core sequence of the N gene TRS (boxed) are shown together with the structure and size of the HCoV-229E genome. The HCoV-229E nt ^{25671}AAA^{25673} within the TRS-N core sequence (underlined) was changed to a random sequence indicated as NNN. (B) An RT-PCR sequencing analysis of in vitro-transcribed HCoV-229E-based genomes with randomized HCoV-229E nt 25671 to 25673 is shown (input genomes) (left). These genomes were used for transfection of BHK-21 cells. Three days later, the poly(A)-containing RNA was isolated and analyzed by RT-PCR sequencing (reisolated genome) (right). Sequencing results are shown for HCoV-229E nt 25663 to 25680, and the region corresponding to the randomized sequence is underlined. (C) RT-PCR products obtained from input genomes or reisolated genomes were cloned and sequenced. The analysis comprised 44 individual plasmid clones corresponding to input genomes and 41 individual plasmid clones corresponding to reisolated genomes. On the basis of the sequence determined at randomized nt 25671 to 25673, the recombinant genomes were placed in one of four groups: group 1, recombinant genomes with the HCoV-229E wild-type sequence (AAA); group 2, recombinant genomes with a 1-nt change compared to the TRS-N or leader-TRS sequence; group 3, recombinant genomes containing a U nucleotide at HCoV-229E position 25673 (NNU); group 4, sequences that do not match to groups 1 to 3. The percentages of each group in the population of input and reisolated genomes are indicated.
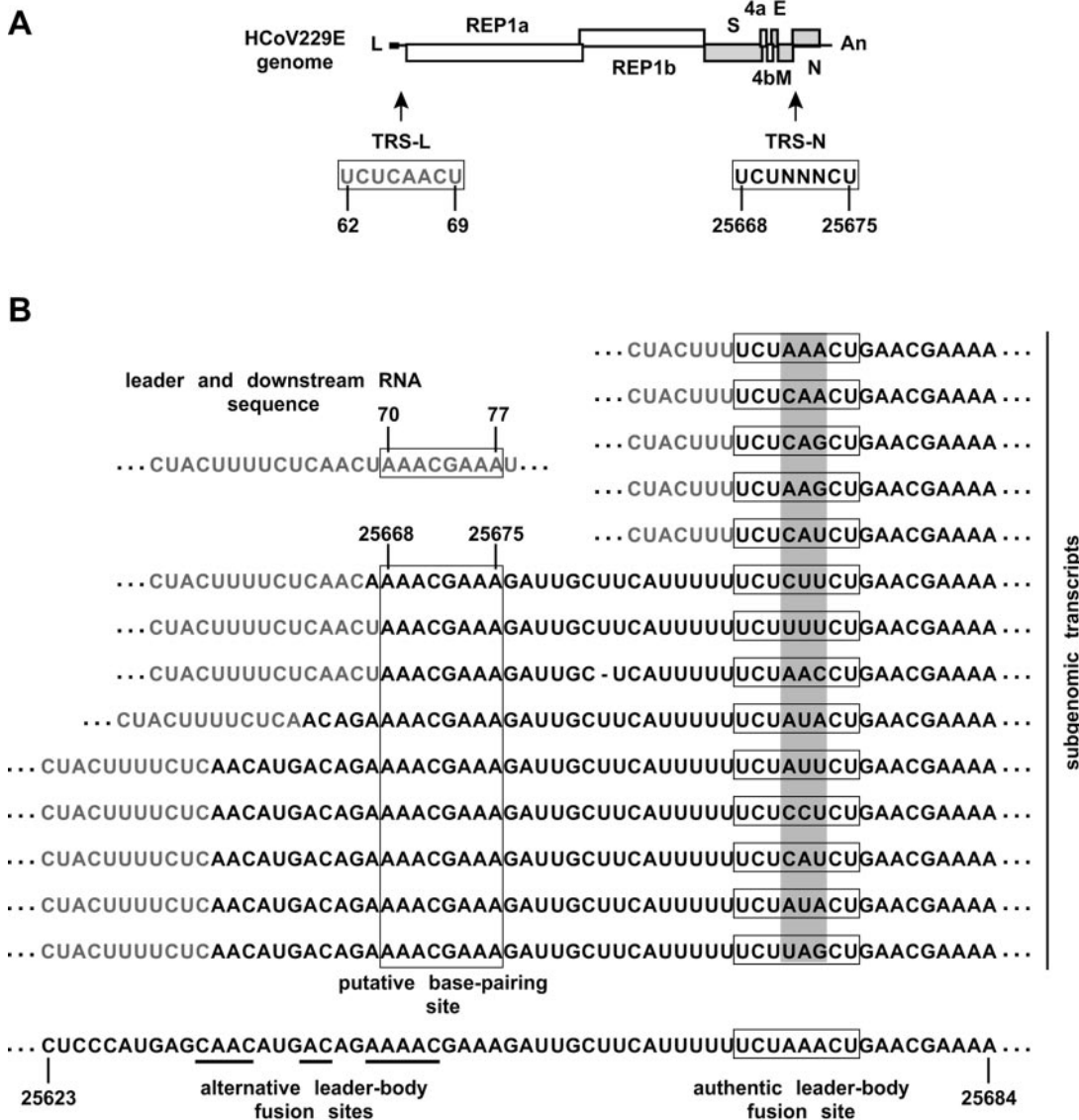
FIG. 6. Sequence analysis of subgenomic N protein mRNAs. (A) The structure and size of the recombinant HCoV-229E genome with randomized nt 25671 to 25673 are shown together with the core sequences of the leader TRS and TRS-N. Numbers indicate nucleotide positions within the HCoV-229E genome. (B) The leader-body junction sequences of subgenomic N protein mRNAs are shown, determined after leader-body-specific RT-PCR sequencing analysis. Leader and body-derived nucleotides are shown in gray and black letters, respectively. For each subgenomic N protein mRNA, the region of the TRS-N core sequence (box) and the sequence corresponding to the randomized nt 25671 to 25673 (shaded in gray) are indicated. For comparison, HCoV-229E nt 55 to 78 encoding part of the leader RNA and downstream sequences (top left) and the HCoV-229E nt 25623 to 25684 containing the TRS-N and flanking regions are shown (bottom). Also highlighted are two stretches of 8 nt encoded downstream of the leader TRS (nt 70 to 77) and upstream of the TRS-N (nt 25668 to 25674) that might be involved in base pairing during discontinuous extension (see Discussion). Alternative leader-body fusion sites are underlined.

UCUCAUCU, contained a uridine at position 25673). Interestingly, however, we could also determine nine N protein mRNA sequences that appeared to contain alternative leader-body fusion sites, although each of these mRNAs was only found once in our sample. It is noteworthy that eight of these "unusual" N protein mRNAs contained either only one nucleotide change, compared to the leader or N gene TRS, or a uridine at position 25673. Thus, irrespective of which leader-body fusion site had been used for the production of a particular N protein mRNA, 13 of 14 TRS-N elements sequenced in this experiment correlated with HCoV-229E genomes that had

undergone a positive selection or remained at the same level during their passage in BHK-21 cells.

DISCUSSION

The overall conclusion of this study is that expression of the coronavirus N protein facilitates replication of the genomic RNA. This is true for N protein that is provided in *trans* during the earliest stages of infection (which may be equivalent to N protein brought into the cell as part of the viral nucleocapsid) or N protein that is expressed from a replicase-transcriptase

complex in the context of a coronavirus-based replicon or an infectious coronavirus genome. This conclusion is based upon evidence resulting from transfection experiments using coronavirus-based vector RNAs and genetic evidence using recombinant, full-length coronavirus genomes. Most notably, transfection of coronavirus-based vector RNAs revealed that we can only detect the amplification of full-length, HCoV-229E-derived vector RNAs in transfected cells if they encode a functional N protein gene or if sustained N protein expression is ensured in *trans* (e.g., mediated by coreplicating virus). In contrast, subgenomic mRNA transcripts were readily detectable, irrespective of the presence or absence of the N gene in the vector RNA. The genetic evidence is that HCoV-229E genomes that are able to express N protein confer a selective advantage for replication in nonpermissive cells. This does not mean that genomes that are unable to express N protein will not replicate if N protein is provided in *trans*, but in a transfection experiment where only a small percentage of cells establish a functional replicase/transcriptase complex, the selective advantage conferred by N protein expression will be more evident. Also, our finding that the PEDV N protein but not the MHV N protein can at least partially reproduce the effects seen with the HCoV-229E N protein suggests that the HCoV-229E replicase complex or RNA genome can interact with N proteins derived from closely related viruses (e.g., coronaviruses of the same group) but not with N proteins from more distantly related viruses.

In addition to the main conclusion, our analysis of the replication of mutated HCoV-229E genomes led to a number of observations that may be relevant to the mechanism of coronavirus transcription. First, it is evident that when the authentic N gene TRS is rendered nonfunctional, the virus is able to use alternative body leader fusion sites. The analysis of alternative leader-body junctions revealed that a stretch of 8 nucleotides located upstream of the TRS-N element (^{25645}AAACGAAA^{25653}) could also be found immediately downstream the leader TRS (^{70}AAACGAAA^{77}), which suggests that base pairing might have taken place at or near to these sequences. The actual leader-body junction sites were determined at body RNA-derived nucleotides ^{25640}AC^{25642}, ^{25634}AAC^{25636}, or ^{25645}AAAC^{25648} (Fig. 6B). Thus, the leader-body junction was either within a putative base-pairing region (as in natural TRS elements) or at adjacent upstream sequences containing AC or AAC nucleotides. In this context, it is interesting that a common feature of the order *Nidovirales* is an open reading frame 1b-encoded protein that has NendoU activity with a strong preference for cleavage at GU(U) sequences in double-stranded RNA substrates (18, 46). It has been suggested that GU(U) sequences at the 3' terminus of nascent minus-strand RNAs, which correspond to conserved AAC nucleotides in the core of the HCoV-229E TRS element, might be substrates of this activity; therefore, NendoU activity might be involved in the transcription of subgenomic mRNAs (18). Our data support the functional importance of the AAC sequence in HCoV-229E TRS elements, but further studies are required to provide a direct link to the activities of enzymes such as the uridylate-specific endoribonuclease.

The data we have presented provide substantial evidence for a functional role of a structural protein in coronavirus RNA synthesis. To our knowledge, this is the first example of a structural protein that is involved in the RNA synthesis of a nonsegmented positive-strand RNA virus. Among all positive-strand RNA viruses, there is only a single group of plant viruses, namely, alfamoviruses and ilarviruses from the *Bromoviridae* family, for which a similar phenomenon has been reported (5, 19, 56). These viruses contain a tripartite positive-strand RNA genome with RNA1- and RNA2-encoding proteins involved in viral RNA replication and RNA3 giving rise to a subgenomic mRNA4 encoding the coat protein. It has been shown that a mixture of three genomic RNAs of alfamoviruses and ilarviruses is not infectious to plants unless the coat protein or mRNA4 is added to the inoculum. This phenomenon has been termed genome activation and appears to take place prior to minus-strand RNA synthesis, most probably through binding of coat protein to conserved RNA structures at the 3' end of the genomic RNAs, resulting in an enhancement of translation (32, 33). In addition, the coat protein is also involved in plus-strand RNA synthesis ("asymmetric plus-strand RNA accumulation"); interestingly, the coat protein is in fact part of the alfamovirus and ilarvirus replication complexes. Although there are striking similarities to the data presented here, further studies are required to elucidate the mechanism(s) of N protein function in coronavirus replication.

In contrast to positive-strand RNA viruses, an involvement of structural proteins in virus replication and transcription has been described for a number of negative-stand RNA viruses, particularly viruses with nonsegmented genomes. *Vesicular stomatitis virus* (VSV; order *Mononegavirales*, family *Rhabdoviridae*) is one of the most advanced experimental systems, and a number of studies related to replication and transcription have been reported (3, 58). For example, it has recently been proposed by Banerjee and colleagues (35) that two distinct polymerase complexes carry out transcription and replication of VSV genomic RNA. The virus proteins L and P (for large protein catalytic subunit and the essential phosphoprotein cofactor, respectively) are part of the transcriptase complex while the L, P, and N proteins are part of the replicase complex. It has also been proposed that the VSV N protein may promote read-through at transcription signals and that VSV replication may require a significant amount of N protein for the encapsidation of the nascent strand. Unlike positive-strand RNA viruses, the template for replication in the case of VSV is a ribonucloprotein complex composed of genome-sized RNAs and the N protein (4). Thus, it appears that in many negative-strand RNA viruses the processes of replication and transcription are tightly regulated by a structural protein. Whether distinct enzyme complexes also distinguish coronavirus replication and transcription and whether the coronavirus N protein has a regulatory role to play in these complexes remain to be determined.

In summary, the present study complements and extends our current understanding of coronavirus replication and transcription. We have identified a structural protein as a factor that facilitates coronavirus genome replication; to the best of our knowledge, this is unprecedented among nonsegmented positive-strand RNA viruses. The functional importance of coronavirus N proteins in fundamental aspects of the coronavirus life cycle, namely encapsidation and replication of virus genomes, suggests that the N protein provides an attractive

target for antiviral intervention aimed at combating coronavirus infections.

REFERENCES

1. **Almazan, F., C. Galan, and L. Enjuanes.** 2004. The nucleoprotein is required for efficient coronavirus genome replication. J. Virol. **78:**12683–12688.
2. **Baric, R. S., G. W. Nelson, J. O. Fleming, R. J. Deans, J. G. Keck, N. Casteel, and S. A. Stohlman.** 1988. Interactions between coronavirus nucleocapsid protein and viral RNAs: implications for viral transcription. J. Virol. **62:**4280–4287.
3. **Barr, J. N., S. P. Whelan, and G. W. Wertz.** 2002. Transcriptional control of the RNA-dependent RNA polymerase of vesicular stomatitis virus. Biochim. Biophys. Acta **1577:**337–353.
4. **Blumberg, B. M., M. Leppert, and D. Kolakofsky.** 1981. Interaction of VSV leader RNA and nucleocapsid protein may control VSV genome replication. Cell **23:**837–845.
5. **Bol, J. F.** 1999. Alfalfa mosaic virus and ilarviruses: involvement of coat protein in multiple steps of the replication cycle. J. Gen. Virol. **80:**1089–1102.
6. **Bridgen, A., M. Duarte, K. Tobler, H. Laude, and M. Ackermann.** 1993. Sequence determination of the nucleocapsid protein gene of the porcine epidemic diarrhoea virus confirms that this virus is a coronavirus related to human coronavirus 229E and porcine transmissible gastroenteritis virus. J. Gen. Virol. **74:**1795–1804.
7. **Casais, R., V. Thiel, S. G. Siddell, D. Cavanagh, and P. Britton.** 2001. Reverse genetics system for the avian coronavirus infectious bronchitis virus. J. Virol. **75:**12359–12369.
8. **Cavanagh, D.** 1995. The coronavirus surface glycoprotein, p. 73–113. *In* S. G. Siddell (ed.), The *Coronaviridae*. Plenum Press, New York, N.Y.
9. **Chang, R. Y., and D. A. Brian.** 1996. *cis* requirement for N-specific protein sequence in bovine coronavirus defective interfering RNA replication. J. Virol. **70:**2201–2207.
9a. **Coley, S. E., E. Lavi, S. G. Sawicki, L. Fu, B. Schelle, N. Karl, S. G. Siddell, and V. Thiel.** 2005. Recombinant mouse hepatitis virus strain A59 from cloned, full-length cDNA replicates to high titers in vitro and is fully pathogenic in vivo. J. Virol. **79:**3097–3106.
10. **Collisson, E. W., M. Zhou, P. Gershon, and J. Jayaram.** 2001. Infectious bronchitis virus nucleocapsid protein interactions with the 3′ untranslated region of genomic RNA depend on uridylate bases. Adv. Exp. Med. Biol. **494:**669–675.
11. **Cologna, R., J. F. Spagnolo, and B. G. Hogue.** 2000. Identification of nucleocapsid binding sites within coronavirus-defective genomes. Virology **277:**235–249.
12. **Denison, M. R., W. J. Spaan, Y. van der Meer, C. A. Gibson, A. C. Sims, E. Prentice, and X. T. Lu.** 1999. The putative helicase of the coronavirus mouse hepatitis virus is processed from the replicase gene polyprotein and localizes in complexes that are active in viral RNA synthesis. J. Virol. **73:**6862–6871.
13. **Fischer, F., C. F. Stegen, P. S. Masters, and W. A. Samsonoff.** 1998. Analysis of constructed E gene mutants of mouse hepatitis virus confirms a pivotal role for E protein in coronavirus assembly. J. Virol. **72:**7885–7894.
14. **Herold, J., T. Raabe, and S. Siddell.** 1993. Molecular analysis of the human coronavirus (strain 229E) genome. Arch. Virol. Suppl. **7:**63–74.
15. **Hertzig, T., E. Scandella, B. Schelle, J. Ziebuhr, S. G. Siddell, B. Ludewig, and V. Thiel.** 2004. Rapid identification of coronavirus replicase inhibitors using a selectable replicon RNA. J. Gen. Virol. **85:**1717–1725.
16. **Heusipp, G., C. Grotzinger, J. Herold, S. G. Siddell, and J. Ziebuhr.** 1997. Identification and subcellular localization of a 41 kDa, polyprotein 1ab processing product in human coronavirus 229E-infected cells. J. Gen. Virol. **78:**2789–2794.
17. **Huang, P., and M. M. Lai.** 2001. Heterogeneous nuclear ribonucleoprotein a1 binds to the 3′-untranslated region and mediates potential 5′-3′-end cross talks of mouse hepatitis virus RNA. J. Virol. **75:**5009–5017.
18. **Ivanov, K. A., T. Hertzig, M. Rozanov, S. Bayer, V. Thiel, A. E. Gorbalenya, and J. Ziebuhr.** 2004. Major genetic marker of nidoviruses encodes a replicative endoribonuclease. Proc. Natl. Acad. Sci. USA **101:**12694–12699.
19. **Jaspars, E. M.** 1999. Genome activation in alfamo- and ilarviruses. Arch. Virol. **144:**843–863.
20. **Kocherhans, R., A. Bridgen, M. Ackermann, and K. Tobler.** 2001. Completion of the porcine epidemic diarrhoea coronavirus (PEDV) genome sequence. Virus Genes **23:**137–144.
21. **Li, H. P., P. Huang, S. Park, and M. M. Lai.** 1999. Polypyrimidine tract-binding protein binds to the leader RNA of mouse hepatitis virus and serves as a regulator of viral transcription. J. Virol. **73:**772–777.
22. **Masters, P. S.** 1992. Localization of an RNA-binding domain in the nucleocapsid protein of the coronavirus mouse hepatitis virus. Arch. Virol. **125:**141–160.
23. **Merchlinsky, M., and B. Moss.** 1992. Introduction of foreign DNA into the vaccinia virus genome by in vitro ligation: recombination-independent selectable cloning vectors. Virology **190:**522–526.
24. **Molenkamp, R., and W. J. Spaan.** 1997. Identification of a specific interaction between the coronavirus mouse hepatitis virus A59 nucleocapsid protein and packaging signal. Virology **239:**78–86.
25. **Molenkamp, R., H. van Tol, B. C. Rozier, Y. van der Meer, W. J. Spaan, and E. J. Snijder.** 2000. The arterivirus replicase is the only viral protein required for genome replication and subgenomic mRNA transcription. J. Gen. Virol. **81:**2491–2496.
26. **Nanda, S. K., R. F. Johnson, Q. Liu, and J. L. Leibowitz.** 2004. Mitochondrial HSP70, HSP40, and HSP60 bind to the 3′ untranslated region of the murine hepatitis virus genome. Arch. Virol. **149:**93–111.
27. **Nanda, S. K., and J. L. Leibowitz.** 2001. Mitochondrial aconitase binds to the 3′ untranslated region of the mouse hepatitis virus genome. J. Virol. **75:**3352–3362.
28. **Narayanan, K., C. J. Chen, J. Maeda, and S. Makino.** 2003. Nucleocapsid-independent specific viral RNA packaging via viral envelope protein and viral RNA signal. J. Virol. **77:**2922–2927.
29. **Narayanan, K., K. H. Kim, and S. Makino.** 2003. Characterization of N protein self-association in coronavirus ribonucleoprotein complexes. Virus Res. **98:**131–140.
30. **Narayanan, K., A. Maeda, J. Maeda, and S. Makino.** 2000. Characterization of the coronavirus M protein and nucleocapsid interaction in infected cells. J. Virol. **74:**8127–8134.
31. **Narayanan, K., and S. Makino.** 2001. Cooperation of an RNA packaging signal and a viral envelope protein in coronavirus RNA packaging. J. Virol. **75:**9059–9067.
32. **Neeleman, L., H. J. Linthorst, and J. F. Bol.** 2004. Efficient translation of alfamovirus RNAs requires the binding of coat protein dimers to the 3′ termini of the viral RNAs. J. Gen. Virol. **85:**231–240.
33. **Neeleman, L., R. C. Olsthoorn, H. J. Linthorst, and J. F. Bol.** 2001. Translation of a nonpolyadenylated viral RNA is enhanced by binding of viral coat protein or polyadenylation of the RNA. Proc. Natl. Acad. Sci. USA **98:**14286–14291.
34. **Nelson, G. W., S. A. Stohlman, and S. M. Tahara.** 2000. High affinity interaction between nucleocapsid protein and leader/intergenic sequence of mouse hepatitis virus RNA. J. Gen. Virol. **81:**181–188.
35. **Qanungo, K. R., D. Shaji, M. Mathur, and A. K. Banerjee.** 2004. Two RNA polymerase complexes from vesicular stomatitis virus-infected cells that carry out transcription and replication of genome RNA. Proc. Natl. Acad. Sci. USA **101:**5952–5957.
36. **Raamsman, M. J., J. K. Locker, A. de Hooge, A. A. de Vries, G. Griffiths, H. Vennema, and P. J. Rottier.** 2000. Characterization of the coronavirus mouse hepatitis virus strain A59 small membrane protein E. J. Virol. **74:**2333–2342.
37. **Rinck, G., C. Birghan, T. Harada, G. Meyers, H.-J. Thiel, and N. Tautz.** 2001. A cellular J-domain protein modulates polyprotein processing and cytopathogenicity of a pestivirus. J. Virol. **75:**9470–9482.
38. **Risco, C., I. M. Anton, L. Enjuanes, and J. L. Carrascosa.** 1996. The transmissible gastroenteritis coronavirus contains a spherical core shell consisting of M and N proteins. J. Virol. **70:**4773–4777.
39. **Sawcki, S. G., and D. L. Sawicki (ed.).** 2005. Coronavirus transcription: a perspective, vol. 287. Springer, Berlin, Germany.
40. **Sawicki, S. G., and D. L. Sawicki.** 1990. Coronavirus transcription: subgenomic mouse hepatitis virus replicative intermediates function in RNA synthesis. J. Virol. **64:**1050–1056.
41. **Sawicki, S. G., and D. L. Sawicki.** 1998. A new model for coronavirus transcription. Adv. Exp. Med. Biol. **440:**215–219.
42. **Sethna, P. B., M. A. Hofmann, and D. A. Brian.** 1991. Minus-strand copies of replicating coronavirus mRNAs contain antileaders. J. Virol. **65:**320–325.
43. **Shi, S. T., G. Y. Yu, and M. M. Lai.** 2003. Multiple type A/B heterogeneous nuclear ribonucleoproteins (hnRNPs) can replace hnRNP A1 in mouse hepatitis virus RNA synthesis. J. Virol. **77:**10584–10593.
44. **Siddell, S. G., J. Ziebuhr, and E. J. Snijder.** 2005. Coronaviruses, toroviruses and arteriviruses. *In* B. W. J. Mahy and V. ter Meulen (ed.), Topley and Wilson's Microbiology and Microbial Infections, 10th ed., vol. 1 and 2, in press. Edward Arnold, London, United Kingdom.
45. **Sims, A. C., J. Ostermann, and M. R. Denison.** 2000. Mouse hepatitis virus replicase proteins associate with two distinct populations of intracellular membranes. J. Virol. **74:**5647–5654.
46. **Snijder, E. J., P. J. Bredenbeek, J. C. Dobbe, V. Thiel, J. Ziebuhr, L. L. Poon, Y. Guan, M. Rozanov, W. J. Spaan, and A. E. Gorbalenya.** 2003. Unique and conserved features of genome and proteome of SARS-coronavirus, an early split-off from the coronavirus group 2 lineage. J. Mol. Biol. **331:**991–1004.

47. **Spaan, W., H. Delius, M. Skinner, J. Armstrong, P. Rottier, S. Smeekens, B. A. van der Zeijst, and S. G. Siddell.** 1983. Coronavirus mRNA synthesis involves fusion of non-contiguous sequences. EMBO J. **2:**1839–1844.

48. **Stohlman, S. A., R. S. Baric, G. N. Nelson, L. H. Soe, L. M. Welter, and R. J. Deans.** 1988. Specific interaction between coronavirus leader RNA and nucleocapsid protein. J. Virol. **62:**4288–4295.

49. **Thiel, V., J. Herold, B. Schelle, and S. G. Siddell.** 2001. Infectious RNA transcribed in vitro from a cDNA copy of the human coronavirus genome cloned in vaccinia virus. J. Gen. Virol. **82:**1273–1281.

50. **Thiel, V., J. Herold, B. Schelle, and S. G. Siddell.** 2001. Viral replicase gene products suffice for coronavirus discontinuous transcription. J. Virol. **75:** 6676–6681.

51. **Thiel, V., K. A. Ivanov, A. Putics, T. Hertzig, B. Schelle, S. Bayer, B. Weissbrich, E. J. Snijder, H. Rabenau, H. W. Doerr, A. E. Gorbalenya, and J. Ziebuhr.** 2003. Mechanisms and enzymes involved in SARS coronavirus genome expression. J. Gen. Virol. **84:**2305–2315.

52. **Thiel, V., N. Karl, B. Schelle, P. Disterer, I. Klagge, and S. G. Siddell.** 2003. Multigene RNA vector based on coronavirus transcription. J. Virol. **77:**9790–9798.

53. **Thiel, V., A. Rashtchian, J. Herold, D. M. Schuster, N. Guan, and S. G. Siddell.** 1997. Effective amplification of 20-kb DNA by reverse transcription PCR. Anal. Biochem. **252:**62–70.

54. **Thiel, V., and S. G. Siddell.** 1994. Internal ribosome entry in the coding region of murine hepatitis virus mRNA 5. J. Gen. Virol. **75:**3041–3046.

55. **van der Meer, Y., E. J. Snijder, J. C. Dobbe, S. Schleich, M. R. Denison, W. J. Spaan, and J. K. Locker.** 1999. Localization of mouse hepatitis virus nonstructural proteins and RNA synthesis indicates a role for late endosomes in viral replication. J. Virol. **73:**7641–7657.

56. **van der Vossen, E. A., L. Neeleman, and J. F. Bol.** 1994. Early and late functions of alfalfa mosaic virus coat protein can be mutated separately. Virology **202:**891–903.

57. **van Marle, G., J. C. Dobbe, A. P. Gultyaev, W. Luytjes, W. J. Spaan, and E. J. Snijder.** 1999. Arterivirus discontinuous mRNA transcription is guided by base pairing between sense and antisense transcription-regulating sequences. Proc. Natl. Acad. Sci. USA **96:**12056–12061.

58. **Whelan, S. P., J. N. Barr, and G. W. Wertz.** 2004. Transcription and replication of nonsegmented negative-strand RNA viruses. Curr. Top. Microbiol. Immunol. **283:**61–119.

59. **Yount, B., K. M. Curtis, and R. S. Baric.** 2000. Strategy for systematic assembly of large RNA and DNA genomes: transmissible gastroenteritis virus model. J. Virol. **74:**10600–10611.

60. **Ziebuhr, J., E. J. Snijder, and A. E. Gorbalenya.** 2000. Virus-encoded proteinases and proteolytic processing in the Nidovirales. J. Gen. Virol. **81:**853–879.

61. **Zuniga, S., I. Sola, S. Alonso, and L. Enjuanes.** 2004. Sequence motifs involved in the regulation of discontinuous coronavirus subgenomic RNA synthesis. J. Virol. **78:**980–994.